

# Statistical mechanics characterization of neuronal mosaics

Luciano da Fontoura Costa\*

*Instituto de Física de São Carlos, Universidade de São Paulo,  
Av. Trabalhador São Carlense 400, Caixa Postal 369,  
CEP 13560-970, São Carlos, São Paulo, Brazil*

Fernando Rocha and Silene Maria Araújo de Lima

*Centro de Ciências Biológicas, Departamento de Fisiologia,  
Universidade Federal do Pará, Campus Universitário do Guamá,  
Rua Augusto Corrêa 01, CEP 66075-000, Belém, Pará, Brazil*

(Dated: 3rd November 2004)

## Abstract

The spatial distribution of neuronal cells is an important requirement for achieving proper neuronal function in several parts of the nervous system of most animals. For instance, specific distribution of photoreceptors and related neuronal cells, particularly the ganglion cells, in mammal's retina is required in order to properly sample the projected scene. This work presents how two concepts from the areas of statistical mechanics and complex systems, namely the *lacunarity* and the *multiscale entropy* (i.e. the entropy calculated over progressively diffused representations of the cell mosaic), have allowed effective characterization of the spatial distribution of retinal cells.

---

\*Electronic address: luciano@if.sc.usp.br

Although a great part of neuronal function is a consequence of the distribution and adaptation of the involved synaptic weights, the topographical nature of sensory spaces found in several animals implies the spatial distribution of neuronal cells to become an important element for achieving proper overall behavior of neuronal subsystems [1, 2]. The topographical organization of neuronal systems and mappings is characterized by the preservation of local adjacencies of the represented and mapped points (e.g. [3]). In the retina, for instance, the photoreceptors and associated neuronal cells are spatially organized as *mosaics* so as to obtain proper sampling of the projected images, which may depend on the specific spectral range and type of visual operation (e.g. central/peripheric and chromatic/scotopic). More specifically, while such a distribution tends to lead to locally uniform distribution of receptive fields, with just the right amount of overlap, the overall distribution varies with the eccentricity, becoming less dense at the paraphoveal regions and periphery of the retina.

At the same time, retinae of several species involve more than one type of photoreceptors, specialized at some particular wavelength interval, implying additional restrictions to the spatial distributions in each respective mosaic. Combined with the close relationship between neuronal structure and function, such specific demands makes the problem of mosaic spatial characterization particularly interesting from both the mathematical and physiological points of view. At the same time, most related researches reported in the specific literature are almost invariably related to the application of nearest-neighbor distances between the mosaic elements. Although such a measurement is interesting and has paved the way to several advances, the consideration of additional, complementary features to describe the spatial organization has the potential to provide more information about the investigated systems.

This article describes the application, to our best knowledge for the first time, of two concepts derived from statistical mechanics and complex systems — namely the lacunarity and multiscale entropy — to the characterization of retinal mosaics.

Introduced [4, 5, 6, 7] in order to complement the degenerated characterization provided by the fractal dimension, the *lacunarity* provides a measurement of the *translational invariance* of the analyzed spatial distributions. Therefore, the higher the value of the lacunarity, the less translationally invariant is the system. Let the sum of the mosaic values under the

circular area of radius  $r$  centered at each point  $(x, y)$ , represented as  $\phi$ , be

$$s_r(x, y) = \sum_{\phi} a(x, y) \quad (1)$$

where  $a$  is the matrix representing the mosaic. One of the frequently adopted definitions of lacunarity is as follows

$$L(r) = \frac{\sigma_r^2}{\mu_r^2} \quad (2)$$

where  $\mu_r$  and  $\sigma_r$  are the mean and standard deviation of  $s_r(x, y)$  taken along the  $xy$  domain. Observe that the lacunarity maps the image into the vector  $L(r)$ ,  $r = 1, 2, \dots, r_{max}$ . For enhanced computation sake, the lacunarity was obtained by convolving, in the spectral domain, the original mosaic with disks of increasing radius.

The multiscale entropy [8, 9] can be used to complement the degeneracy of the traditional entropy, which is invariant to any spatial permutation of the mosaic values (the entropy ultimately depends only on the image value histogram which, as a first order statistics, does not depend on the spatial positions). More specifically, the multiscale entropy can be defined as follows

$$E_{\sigma} = - \sum_v p_{\sigma}(v) \log(p_{\sigma}(v)) \quad (3)$$

where  $p_{\sigma}(v)$  is the histogram of the mosaic values after diffusion with standard deviation  $\sigma$  (e.g. Gaussian smoothing, which is equivalent to linear isotropic diffusion). The diffused versions of the original mosaic images were obtained through the convolution, in the spectral domain, of the original mosaic image with normal density functions for increasing values of  $\sigma$  [8].

The remainder of this article presents the application of the two above measurements to the characterization of Agouti (*Dasiprocta agouti*) retinal mosaics, which involve two types of cells (M/L and S) characterized by different pigments. The process of enucleation and fixation of the retinal material followed the protocols described elsewhere [10]. Isolated retinas were prepared as whole mounts and were then labeled with different antibodies (JH-455, against S cone pigments and JH-492 against M/L cone pigments; kindly provided by Dr. J. Nathans) largely according to the procedures described elsewhere (\*). The whole-mounted retinas were examined and scanned using differential interference contrast (DIC)

with the aid of an optical microscope (LEICA DM) equipped with a high-resolution video camera (AxionCam MRm). Starting from the optic nerve, images of S and M/L cones were acquired along the vertical-dorsal axis. Using 40X oil immersion objective, 25 fields taken with  $250 \times 250\mu m$  for M/L cones and 23 fields with  $500 \times 500\mu m$  for S cones were digitalized. The raw images of the cones were captured at the level of the inner segments. For analysis,  $x$  and  $y$  coordinates were identified with Scion Image Software (ScionCorp). Digital binary images were then obtained (cells are represented by 1 and absence of cells by 0) and represented as matrices of fixed size 250 (the coordinates of S cones were divided by 2) in order to normalize finite-size effects. Typical examples of the M/L and S cell distributions are provided in Figure 1(a) and (b), respectively.

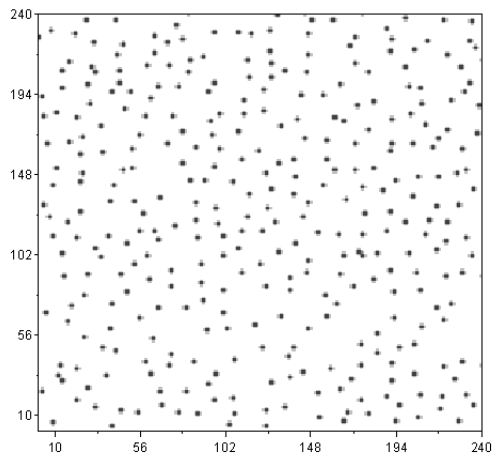
Figure 1(c) presents the scatterplot considering the mean lacunarity and mean multiscale-entropy obtained for each mosaic. It is clear from this figure that both M/L and S cells resulted linearly separated, in the sense that most cases above the dashed line are S cells. The two exceptions were found to have uncommon features. All cells below the line are M/L cells. Because the separation line is almost horizontal and orthogonal to the  $y$ -axis, it follows that such a discrimination is obtained mostly as a consequence of the mean lacunarity measurements. Indeed, as can be inferred from Figures 1(a) and (b), the M/L mosaics tend to be spatially more uniform, implying higher translational invariance. On the other hand, the S mosaics tend to have greater variation as for the size and shape of their void regions, leading to higher lacunarity. Although the mean multiscale entropy did not contribute to separating between M/L and S mosaics, it did produce an isolated cluster at the left-hand side of the figure, which is marked by the ellipse. The mosaics in that cluster have been verified to have a smaller number of cells, a property which was properly reflected by the multiscale entropy.

All in all, we have shown that lacunarity and multiscale entropy measurements derived from digital images of retinal mosaics can provide valuable information about the spatial distribution of the involved cells. While the mean lacunarity accounted for an almost perfect separation of the two types of mosaics, the mean multiscale entropy allowed the identification of a separated cluster of M/L mosaics. Such results provide circumstantial evidence in favor of the fact that irregular rather than regular patterns appear to be the rule among mammals with S cone mosaics [11]. Random distribution in the S cone mosaics have been identified in species like marsupials, rabbits, cats, horses, rats, cheetahs and guinea pigs [10, 12, 13, 14, 15]

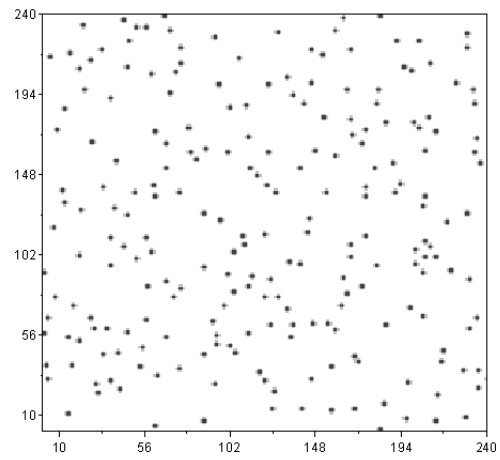
which, like the agouti, have rod-dominant retina. On the other hand, regular S mosaics are found only in animals with cone-dominant retina [16, 17, 18], possibly accounting for enhanced visual sampling properties compatible with diurnal arboreal habitats.

### **Acknowledgments**

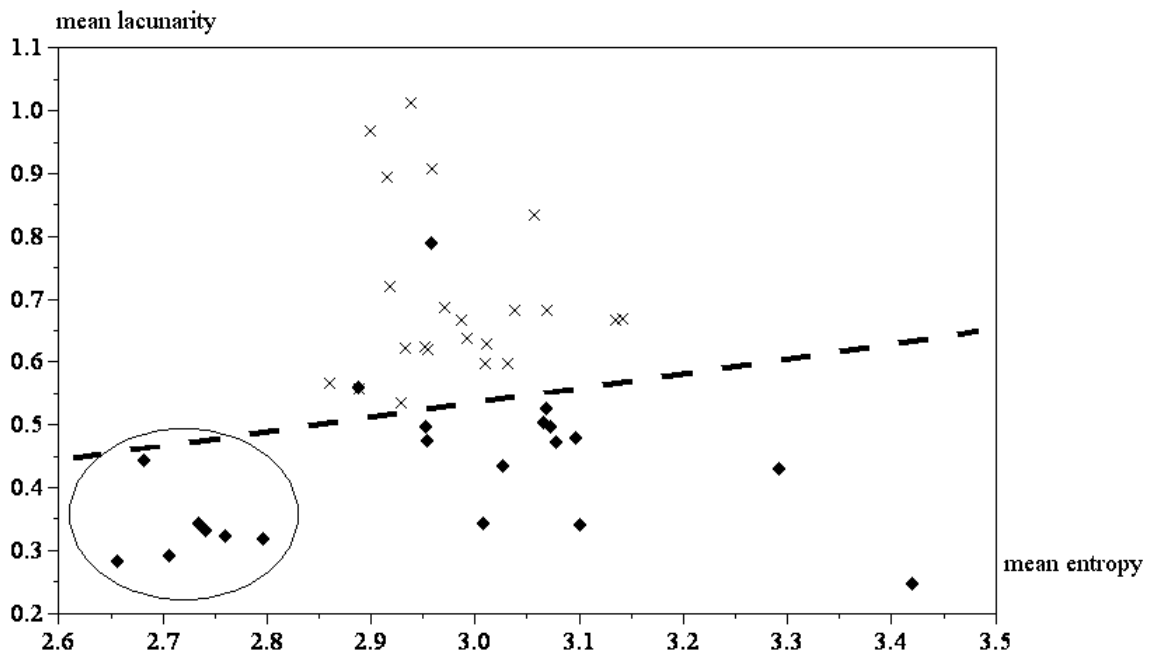
Luciano da F. Costa thanks HFSP RGP39/2002, FAPESP (proc. 99/12765-2) and CNPq (proc. 3082231/03-1) for financial support.



(a)



(b)



(c)

FIG. 1: Figure 1.

List of Captions:

Typical configurations of M/L (a) and S (b) mosaics, and the scatterplot obtained for mean lacunarity and mean entropy (c). M/L and S mosaics are represented by crosses and diamonds, respectively.

- 
- [1] G. H. Jacobs, *Biol. Rev. Camb. Philos. Soc.* **68**, 413 (1993).
- [2] A. Szel, A. Lukats, T. Fetke, Z. Szepessy, and P. Rohlich, *J. Opt. Soc. Am. A Opt. Image Sci. Vis.* **17**, 568 (2000).
- [3] L. da F. Costa and L. Diambra, *Phys. Rev. E* (2004), cond-mat/0305010, accepted.
- [4] Y. Gefen, Y. Meir, B. B. Mandelbrot, and A. Aharony, *Phys. Rev. Letts.* **50**, 145 (1983).
- [5] J.-P. Hovi, A. Aharony, D. Stauffer, and B. B. Mandelbrot, *Phys. Rev. Letts.* **77**, 877 (1996).
- [6] C. Allain and M. Cloitre, *Phys. Rev. A* **44**, 3552 (1991).
- [7] A. J. Einstein, H. S. Wu, and J. Gil, *Phys. Rev. Letts.* **80**, 387 (1998).
- [8] L. da F. Costa and R. M. C. Jr, *Shape Analysis and Classification: Theory and Practice* (CRC Press, Boca Raton, 2001).
- [9] O. M. Bruno, R. M. Cesar, L. A. Consularo, and L. da F. Costa, in *Proc. International Symposium on Computer Graphics, Image Processing and Vision, SIBGRAPI* (IEEE Computer Society Press, Rio de Janeiro, RJ, 1998), vol. 18, pp. 363–370.
- [10] P. K. Ahnelt, J. N. Hokoc, and P. Rohlich, *Vis. Neurosc.* **12**, 793 (1995).
- [11] P. K. Ahnelt and H. Kolb, *Prog. Retin. Eye Res.* **19**, 711 (2000).
- [12] D. Sandmann, B. B. Boycott, and L. Peichl, *J. Neurosc.* **16**, 3381 (1996).
- [13] A. Szel, P. Rohlich, A. R. Caffè, B. Juliusson, G. Aguirre, and T. van Veen, *J. Comp. Neurol.* **325**, 327 (1992).
- [14] P. K. Ahnelt, E. Fernandez, O. Martinez, and A. Kubber-Heiss, *J. Opt. Soc. Am. A* **17**, 580 (2000).
- [15] A. Szel and P. Rohlich, *Exp. Eye Res.* **55**, 47 (1992).
- [16] B. Muller and L. Peichl, *J. Comp. Neurol.* **282**, 581 (1989).
- [17] P. K. Ahnelt, *Vis. Res.* **25**, 1557 (1985).
- [18] K. O. Long and S. K. Fisher, *J. Comp. Neurol.* **221**, 329 (1983).